Indian Journal of Chemistry
Vol. 62, June 2023, pp. 559-567
DOI: 10.56042/ijc.v62i6.2511

Evaluation of drug likeliness of (Z)-4-((4-hydroxy-3-methoxy benzylidene)amino)-1,5-dimethyl-2-phenyl-1,2-dihydro-3*H*-pyrazol-3-one by computational analysis against coronavirus and T-cells of immune system

Gowri M*[a] & Athimoolam S[b]

[a] Department of Chemistry, Avinashilingam Institute for Home Science and Higher Education for Women, Coimbatore 641 043, Tamil Nadu, India

[b] Department of Physics, University College of Engineering (Anna University Constituent College), Konam, Nagercoil 629 004, Tamil Nadu, India

E-mail: sriadit.gowrisuresh@gmail.com, athi81s@yahoo.co.in

Received 21 April 2022; accepted (revised) 19 May 2023

The Schiff base (Z)-4-((4-hydroxy-3-methoxy benzylidene)amino)-1,5-dimethyl-2-phenyl-1,2-dihydro-3*H*-pyrazole-3-one (VAP) has been synthesized by the condensation of 4-aminoantipyrine with vanillin and and characterized by FT-IR, ^{1}H and ^{13}C NMR spectroscopy. The structure of the synthesized compound has been confirmed by single-crystal X-ray diffraction studies, which shows that four units of the compound are in an asymmetric part of the crystal structure. The potential activity of synthesized Schiff base compound has been determined by molecular docking with T-cells (6bnk) and against Coronavirus (6lu7).

Keywords: Vanillin, 4-Aminoantipyrine, Crystal structure, TCR-MHC-like molecule, Covid-19 main protease

Schiff bases synthesized are from a one-step condensation process with various amines. Aldehydes or ketones (due to their diverse chelating ability) react with transition metals to form Schiff base complexes to make potential drug molecules in the medicinal field and effective catalysts in the industrial field. Inexpensiveness and simplest preparation of Schiff base compounds utilized as an analytical reactant can form stable metal complexes with potential biological activities. Aromatic Schiff base compounds and metal complexes are decompositions, electro-reduction, hydrolysis, and oxygenation reactions[1-5]. Those are the most potent chelators because their azomethine nitrogen atom has a high electron density. Due to this property, they are utilized in a wide range of biological applications, especially antimicrobial, anti-cancer, anti-inflammatory, and anti-tubercular agents, and also used in analytical, clinical, catalysts, corrosion inhibitors, dyes, intermediates in organic synthesis, medicinal, polymer stabilizers, pigments, and pharmacological field[6-12].

4-amino antipyrine is an N-phenyl compound. The $-CH_2$ group is bonded on either side of the polar carbonyl group, which is used to reduce and protect from oxidative stress and prevent diseases such as cancer and microbial diseases[13-16]. 4-amino antipyrine has a strong basic character with a significant dipole moment, a potential donor. Its derivatives are analgesic, antimicrobial, anti-cancer, and anti-inflammatory drugs. 4-amino antipyrine derivatives are strong inhibitors of prostanoids synthesis, platelet thromboxane synthesis, and cyclooxygenase isoenzymes, and those catalyze the rate-limiting step in prostaglandin synthesis[17-20].

Vanillin is an aroma compound and a vital flavoring agent in food industries. It is naturally extracted from vanilla beans, and the synthetic vanillin is prepared by two-step synthesis. It has a wide range of biological, therapeutic, and industrial applications. Vanillin, *o*-vanillin, and isovanillin are three isomeric forms of vanillin. Vanillin and its derivatives have essential properties such as antimutagenic, antimicrobial, antioxidant, anticarcinogenic, and free radical scavenging agent[21-23].

The Schiff base, 4-Amino antipyrine with vanillin, has several biological, clinical, pharmaceutical, and industrial applications. These significant properties of reported Schiff bases significantly motivate working with those compounds. The Schiff base was characterized using FTIR, ^{1}H NMR, and ^{13}C NMR spectroscopy. The single-crystal X-ray diffraction studies determine the crystalline structure and

properties of synthesized Schiff base and molecular docking studies to report compounds against covid-19 and improve T-cell activation. The reported Schiff base (VAP) compared with KRN7000 in 6BNK, Favipiravir, and Hydroxychloroquine in 6LU7 proteins.

Experimental Section

The sharp melting point of the reported Schiff base was determined by using Digital Melting Point Apparatus (Safire) with the help of an open capillary tube under the heating rate of 10°C/min. The Schiff base's Fourier transform-infrared spectrum was recorded in the Tensor 27 spectrometer. ^{1}H NMR (400 MHz) and ^{13}C NMR (100 MHz) spectra were recorded by using Bruker Advance (AC80) instrument. DMSO-d_6 and tetramethyl silane (TMS) as internal standards, and the chemical shift values are recorded in δ (ppm). The compound's elemental analysis (CHN) was analyzed using Thermal Finnigan Elemental Micro Analyzer. The reported Schiff base reaction was monitored by thin-layer chromatography; TLC plates are coated with silica gel.

Synthesis of (Z)-4-((4-hydroxy-3-methoxy benzy lidene)amino)-1, 5-dimethyl-2-phenyl-1, 2-dihydro-3*H*-pyrazol-3-one Schiff base

Approximately 0.76 g (5 mmol) of vanillin dissolved in 30 mL of ethanol and 1.015 g (5 mmol) of 4-amino antipyrine was added. The reaction mixture was refluxed over a water bath for about 3 h at RT, and the reaction was monitored by thin-layer chromatography. The resulting solution is tightly covered after reaction completion and allowed to stand without any disturbance. The synthesized Schiff base separated into shiny yellow needle-like crystals and dried in a vacuum. The yield of the Schiff base is 1.265g (75.09%).

Structure determination of Schiff base by single crystal X-ray diffraction studies

The Schiff base VAP is crystallized by solvent evaporation solution growth technique to get block-type single crystals suitable for X-ray diffraction studies. The crystallographic data collection, using the X-ray with the wavelength of 0.71073 Å, was collected at RT with MoKα radiation using Bruker AXS KAPPA APEX-2 diffractometer equipped with graphite monochromator[24].

Molecular docking

The molecular docking study of the interaction and feasibility of the reported Schiff base compound with TCR-MHC-like molecule, Covid-19 main protease, is carried out. The binding affinity of the compound was predicted in AutoDock 4.2 software. The reported compound structure was drawn in Chem3D 18.2, and the ligand file was saved in PDB (protein data bank) format. The structures of proteins downloaded from the Royal Collaboratory for Structural Bioinformatics (http://www.rcsb.org/pdb/) are named 6bnk and 6lu7. Studies on the compound and proteins, prepared by removing water, adding polar hydrogen atoms, and partial charges, were performed using AutoDock Tools 1.5.6. The binding affinity values were determined from molecular docking using AutoDock Vina 1.1.2, which determines the grid values. The three-dimensional structure of protein-ligand positions are shown by using PyMol software[25].

Results and Discussion

Spectral Characterization

FTIR spectra

The C=N azomethine stretching vibration of the Schiff base was observed strong band at 1620 cm^{-1}. Usually, the carbonyl group absorption is around 1700 cm^{-1}; cyclic five-membered carbonyl absorption of the compound is observed at 1755 cm^{-1}. The aromatic and aliphatic C-O stretching frequencies are 1134 and 1207 cm^{-1}, respectively. The phenolic O-H absorption of the Schiff base is observed at 3174 cm^{-1}. The two different C-N bonds in the pyrazole moiety are observed at 1257 cm^{-1} and 1280 cm^{-1}. The FT-IR spectrum of the reported Schiff base is shown in Fig. 1 [26].

^{1}H NMR spectra

The Schiff base shows multiplet around δ 6.9 – 7.5, representing the presence of phenyl rings in the resultant compound. Three distinct peaks around δ 2.4-3.7 represent three different methyl groups in which two methyl groups are present N-CH_3 protons appear at δ 2.4 (s), and C-CH_3 protons appear at δ 3.12 (s). The third one at δ 3.7 can be accounted for by the presence of the methoxy methyl group, which is attached to an oxygen atom of the vanillin moiety. The proton present in azomethine (CH=N) gives singlet at δ 9.6. ^{1}H NMR spectrum is shown in Fig. 2.

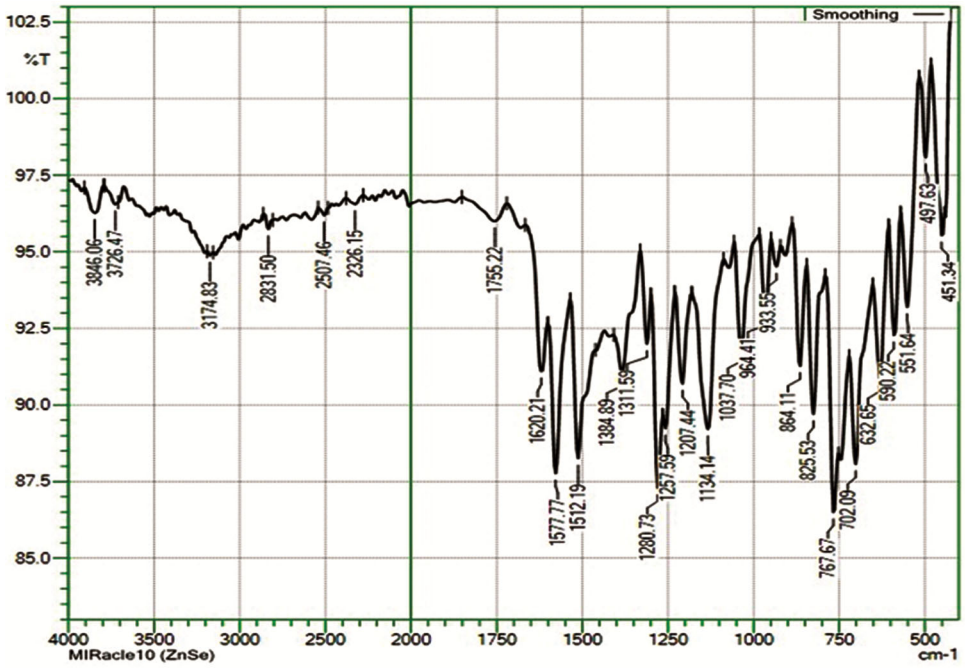

Fig. 1 — FTIR spectrum of the Schiff base

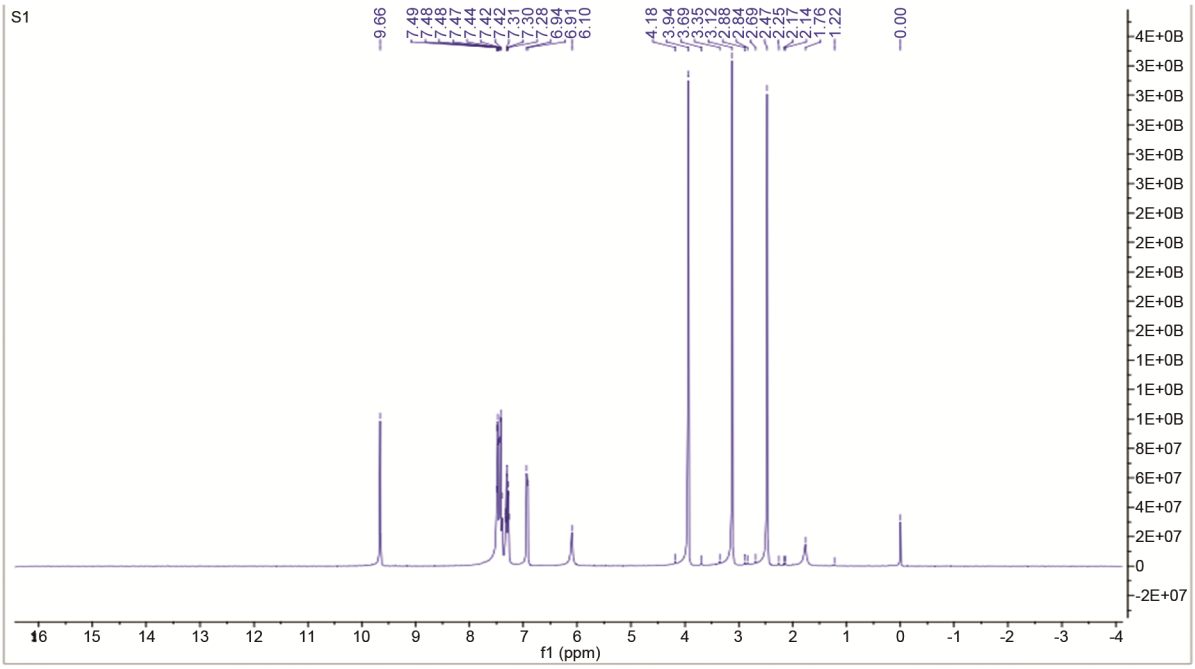

Fig. 2 — ^{1}H NMR spectra of the Schiff base

^{13}C NMR spectra

In the ^{13}C NMR spectrum of the Schiff base, methyl carbons are observed from the peaks at δ 10.12, 35.90, and 55.84. The first two peaks represent methyl groups of antipyrine ring moiety, which are directly attached to the ring carbon and nitrogen atom, and the third peak of a methyl group attached to the oxygen of the phenyl ring. The antipyrine ring carbon atoms appear at δ 148.08 to 151.30. The cluster of peaks from δ 114.36 to 134.78 shows the presence of aromatic carbons in the two phenyl rings of the resulting compound. The carbonyl group and carbon of the azomethine group are present in the resultant Schiff base ligand at δ 157.41 and 160.95,

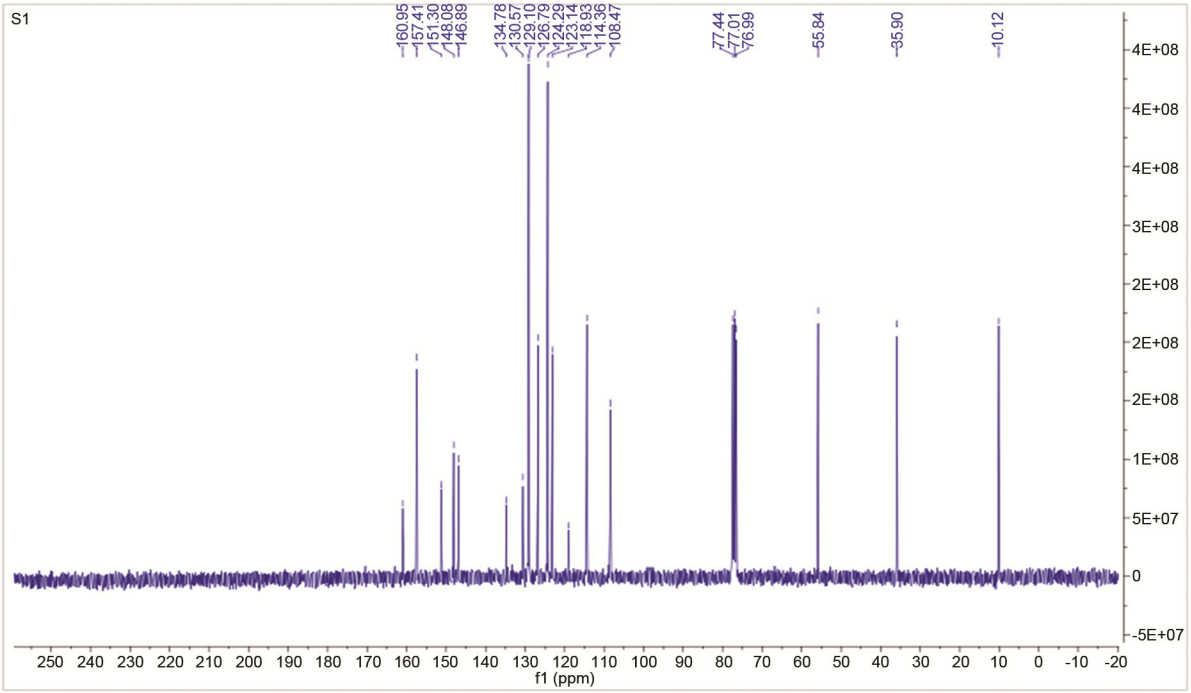

Fig. 3 — ^{13}C NMR spectrum of the Schiff base

respectively. The ^{13}C NMR spectrum is shown in Fig. 3.

Single crystal X-ray diffraction studies

The structure was solved by direct methods and refined by full-matrix least-squares calculations using SHELXL-2014 [27]. All the H atoms were placed at geometrically calculated bond distances, *viz*., -OH = 0.82 Å, -CH = 0.93 Å (for aromatic), and -CH = 0.96 Å (for -CH_3) constrained to ride on the concerned parent atom with Uiso(H) = 1.2 or 1.5 Ueq(parent atom). The crystallographic data, details of data collection, and structure refinement are presented in Table 1. The ORTEP view of the compound plotted at 50% probability thermal displacement ellipsoids with the atom numbering scheme is shown in Fig. 4 [28].

Molecular geometry and crystal packing

The monoclinic non-centrosymmetric C-centered lattice of the Schiff base (VAP) contains four molecules in the unit cell. The R-factor of the refinement (4.58%) confirms the convergent structure. The central five-membered ring makes a dihedral angle of 11.8(1) and 51.1(1)° with the phenyl and disubstituted phenyl rings. Further, the phenyl and disubstituted phenyl rings are oriented at 51.5(1)°. The hydrogen bonding dimensions are listed in

Table 1 — Crystallographic parameters of the Schiff Base VAP

Empirical formula	$C_{19}H_{19}N_3O_3$
Formula weight	337.37
Temperature	293(2) K
Wavelength	0.71073 Å
Crystal system	Monoclinic
Space group	Cc
Unit cell dimensions	a = 11.8124(10) Å b = 16.9998(15) Å c = 8.7869(8) Å
Volume	1738.9(3) Å^3
Z	4
Density (calculated)	1.289 Mg/m^3
Absorption coefficient	0.089 mm^{-1}
F(000)	712
Crystal size	0.25×0.18×0.15 mm^3
Theta range for data collection	2.120 to 28.304°
Index ranges	–15≤h≤15, –22≤k≤22, –11≤l≤11
Reflections collected	10720
Independent reflections	4230 [R(int) = 0.0660]
Completeness to theta	100.00%
Refinement method	Full-matrix least-squares on F^2
Data / restraints / parameters	4230 / 2 / 230
Goodness-of-fit on F^2	0.957
Final R indices [I>2sigma(I)]	R1 = 0.0458, wR2 = 0.1037
R indices (all data)	R1 = 0.0562, wR2 = 0.1087
Absolute structure parameter	0.2(8)
Largest diff. peak and hole	0.158 and –0.206 e.Å^{-3}

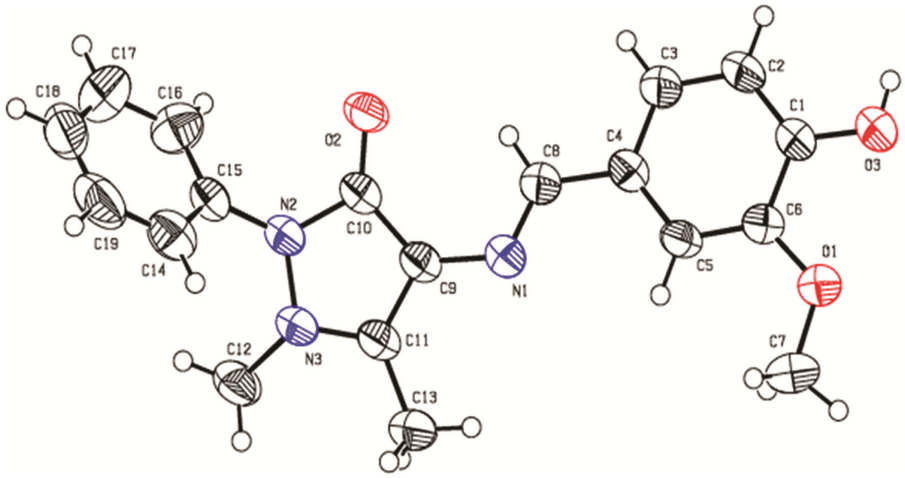

Fig. 4 — Molecular structure of the Schiff base VAP with 50% probability thermal displacement ellipsoids

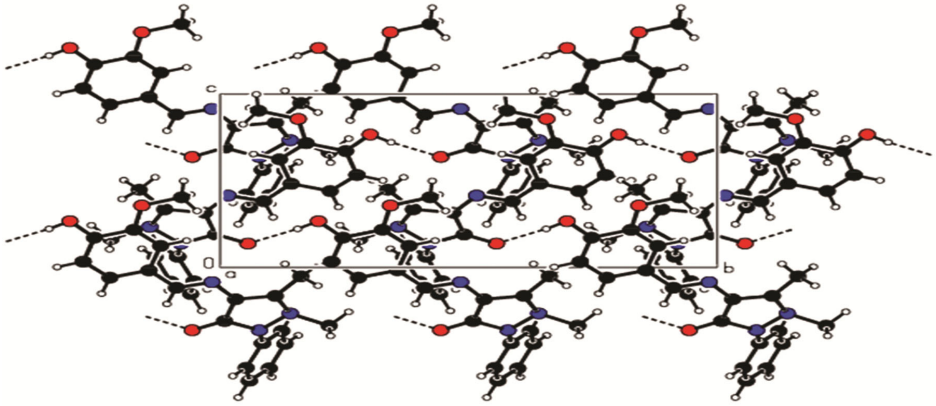

Fig. 5 — Packing of the molecules in triclinic unit cell viewed down along *a*-axis. H-bonds are shown as dashed lines

Table 2 — Hydrogen bonding geometry in the crystal VAP

D-H...A	d(D-H)	d(H...A)	d(D...A)	<(DHA)
C(8)-H(8)...O(2)	0.93	2.38	3.055(4)	128.8
O(3)-H(3)...O(2)$^{\#1}$	0.82	1.87	2.686(3)	174.9
C(7)-H(7B)...N(1)$^{\#2}$	0.96	2.83	3.770(5)	167.9
C(19)-H(19)...O(1)$^{\#3}$	0.93	2.97	3.790(5)	147.2

Table 2, and the packing arrangement of molecules is depicted in Fig. 5. The structure features an intramolecular interaction through C-H…O hydrogen bond with lower energy.

Intermolecular interactions, especially classical and non-classical hydrogen bonds, are crucial in forming crystalline solids and their physiochemical properties. These hydrogen bonding interactions can be classified and notated with graph-set nomenclature, which helps compare the stability of the molecular conformations and crystalline lattices between similar molecules[29]. The crystal packing is stabilized through classical O-H…O hydrogen bonds, non-classical C-H...O, C-H…p, hydrogen bonds, and p-p interactions.

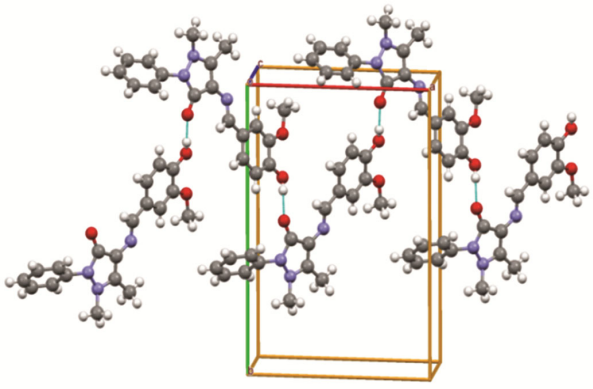

Fig. 6 — O-H…O hydrogen bonds lead to chain C(11) motifs along *a*-axis of the unit cell. H-bonds are shown as dashed lines.

Interestingly, the classical O-H…O hydrogen bond connects the molecules along the *a*-axis of the unit cell in a zig-zag fashion (Fig. 6).

Molecular Docking

Computational chemistry is the mathematical description or chemistry data used to analyze the

Table 3 — Targeted protein molecule and active site of amino acids with the ligand structure

S. No.	Protein data bank ID	Protein chain	Macromolecules	Ligand	Active sites
1	6BNK	CD1d1 and β-2-microglobulin (*Mus musculus*)	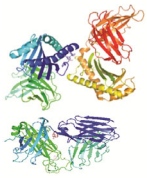	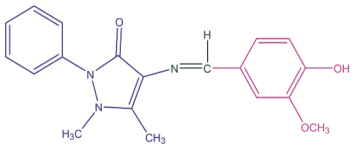	SER114
2	6BNK	Human nkt tcr α-chain and Human nkt tcr β-chain (*Homo sapiens*)	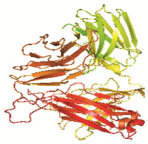	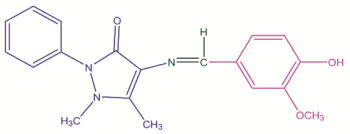	GLN26

Table 4 — Binding affinity comparison of VAP and KRN7000

S. No.	Chains	Binding affinity (Kcal/mol)	
		VAP	KRN7000 (alpha-Galactosylceramide)
1	CD1d1 and β-2-microglobulin (*Mus musculus*)	–7.6	0.0
2	CD1d1 and β-2-microglobulin (*Mus musculus*)	–6.0	0.0

interaction between drug molecules and targeted molecules of microbial, cancer cells, *etc*. Molecular docking is a powerful approach to detecting new structure-based drugs. Molecular docking studies can be done at minimum cost, save time, and and produce fast results in computational studies, which are used to predict the active site, binding angle, binding positions, and binding affinity of the ligand with targeted protein[30,31]. In this research, we are interested in predicting the anti-corona virus activity of our synthesized Schiff base ligand (VAP) by enhancing T-cell activity in the immune system using molecular docking studies on the protein crystal structure of TCR-MHC-like molecule (6bnk) and COVID-19 main protease (6lu7). 3D images of proteins and ligands were derived by PyMol software.

The binding affinity, interactions of drug and protein molecules also, hydrogen bonding of Schiff base (VAP), and protein molecules such as covid-19 (6lu7) and TCR-MHC (6bnk) are determined by using auto dock software. The TCR-MHC-like molecule (6bnk) and COVID-19 main protease (6lu7) crystal structures are downloaded from Royal Collaboratory for Structural Bioinformatics protein data bank.

TCR-MHC-like molecule (6BNK)

The multiple aspects of T cells in the immune system are responses to allergens, pathogens, and tumors. The role of T cells in a mouse model is studied in the specific type of antigen, pathogen, or disease condition over a limited time frame. Human T cells inhibit various diseases and maintain the immune system. T cells are a type of lymphocyte playing a vital role in immune function. Those can vary from other lymphocytes, such as B cells, naturally killing cells. "T" cells mature in the thymus gland, although some are produced in the tonsils. T cells have various types; some T cells are unknown. These can produce cytokines, including interleukins, further stimulating the immune system. There are various methods to activate T cells, such as CAR-T cells. However, our research aimed to activate T cells to improve the immune system and react against covid-19 cells using our reported Schiff base compound[32].

T cell receptor-major histocompatibility complex-like molecules have two parts (*Mus musculus*, *Homo sapiens*) with eight chains, each with four chains. CD1d1 has A, E chains and B, F chains present in beta-2-microglobulin in the *Mus musculus* model also, C, G chains present in Human nkt TCR alpha chain, and Human nkt TCR beta chain has D, H chains in *Homo sapiens* model (Table 3). Our research compared the VAP ligand with KRN7000 glycolipid for *Mus musculus* and *Homo sapiens* in 6BNK (TCR-MHC-like molecule) Table 4 [33]. VAP bound on B pocket of *Mus musculus* and D and G pocket of *Homo sapiens*. VAP compound has bound on B pocket through SER114 with one hydrogen bond interaction (O...H) in *Mus musculus* and one hydrogen bond interaction (O...H) with *Homo sapiens* through GLN26. The Schiff base compound shows the binding position between SER112 to ASN186 in *Mus musculus* and SER68 to GLN73 in *Homo sapiens* (Fig. 7). Comparison between KRN7000 and VAP shows higher binding affinity than KRN7000 in *Mus*

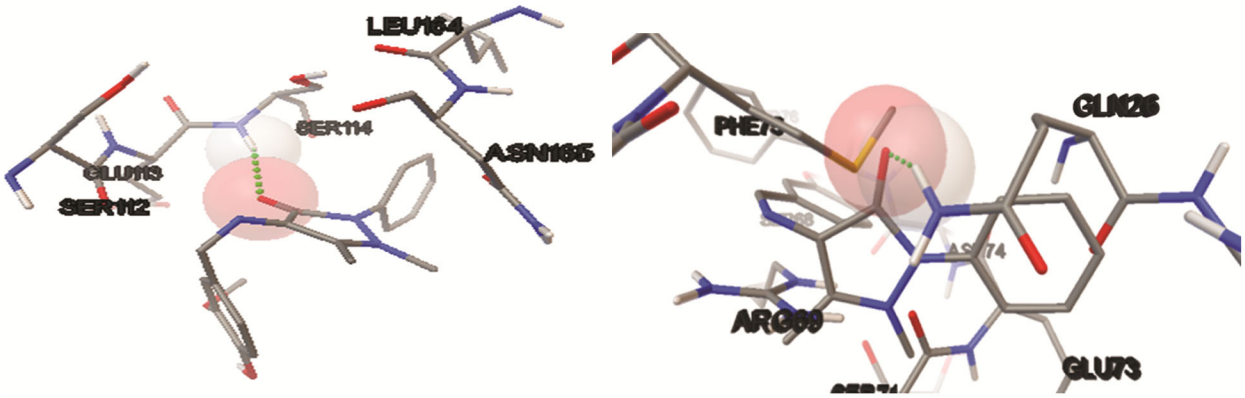

Fig. 7 — Binding position of VAP with receptor 6BNK

Table 5 — Properties of COVID-19 and VAP as a potential inhibitor candidate

S. No	Name of the compound	Molecular formula	Binding site	Lipinski's rule of five	
				Properties	Value
1	VAP	$C_{19}H_{19}N_3O_3$	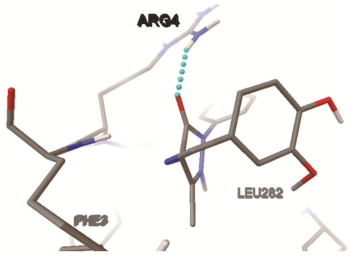	Molecular weight(<500Da)	337.14
				LogP (<5)	1.84
				H-Bond donor (<5)	0
				H-bond acceptor (<10)	1
				Violations	0

musculus and *Homo sapiens*. These binding affinity values show that the VAP compound enhances T-cell activity compared with KRN7000.

COVID-19 main protease (6lu7)

Covid-19 is a viral fever causing respiratory system disease worldwide since 2019, an infectious disease caused by SARS-CoV-2 (severe acute respiratory syndrome coronavirus-2). Currently, there are no drugs to cure this disease, so worldwide; scientists are involved in their research to discover Covid-19 medicine. In recent days, this disease can be cured by using human plasma[34-38].

Covid-19 main protease named 6lu7 were downloaded from the RCSB protein data bank. 6lu7 has one main chain named "A"[39]. The VAP compound was bound on the "A" pocket of 6lu7 using one hydrogen bond through ARG4, and VAP was comparatively studied with Favipiravir and Hydroxychloroquine. Those binding affinities were calculated by using auto dock software. In comparing VAP, Favipiravir, and Hydroxychloroquine, VAP shows excellent binding affinity of –6.7, Favipiravir –5.9, and Hydroxychloroquine –5.2[40]. Lipinsky's rule of five is the thumb rule, which determines whether the chemical compound has excellent pharmacological or biological activity and physical and chemical properties that make it a suitable orally active drug in human beings (Table 5). Lipinski's rule of five accepted the molecular docking study of Schiff base compound.

The negative value of Gibbs free energy of the system shows the spontaneity of the interaction of the Corona Virus protein with the Schiff base VAP. The Gibbs free energy determines the stability of the protein-ligand complex[41], the theoretical IC_{50} value, calculated using binding energy and inhibition constant[42]. The regression graph is drawn from each value of the ligand-receptor complex's binding energy and inhibition constant (ki) (Fig. 8), occurring in a .dlg file using an auto dock. The reason for taking each value of binding energy and inhibition constant of ligand-receptor complex VAP is a single organic compound, so each value is significant to calculate the IC_{50} value.

The estimated Free Energy of Binding is –2.44 kcal/mol, the inhibition constant (ki) is 16.39 mM

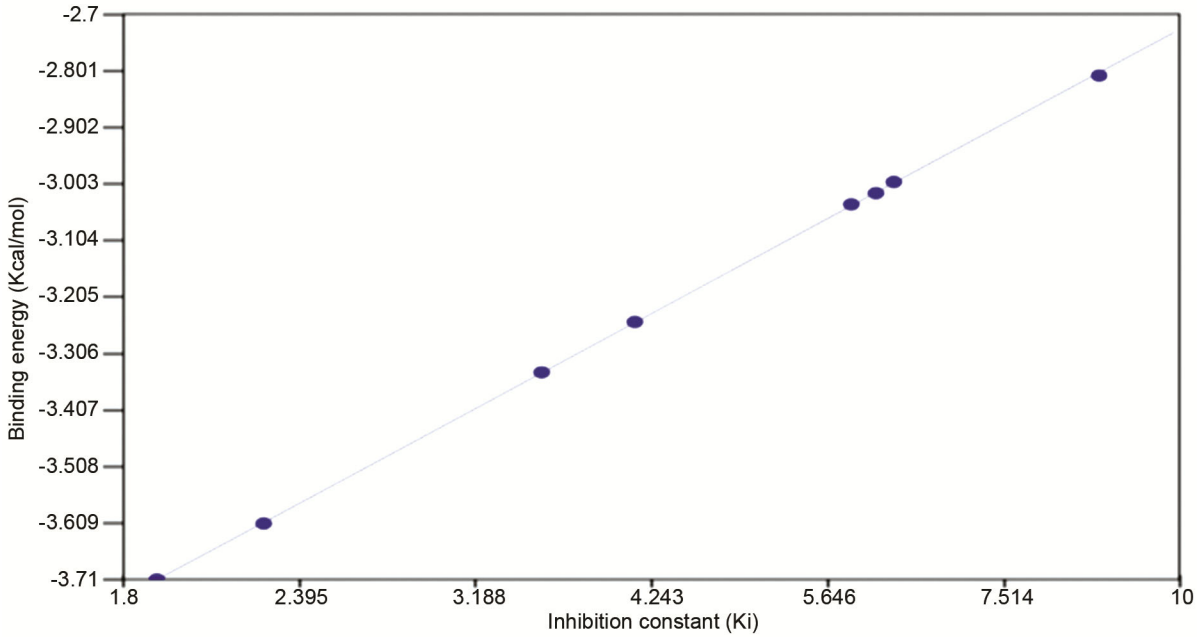

Fig. 8 — IC_{50} regression graph of ligand-receptor complex

(temperature = 298.15 K), the IC_{50} value of ligand-receptor complex is 4.3829 mM, and the regression graph R2 value is 0.9011, which shows the goodness of fit statistic for regression analysis and which means synthesized Schiff base compound has more binding energy with higher inhibition constant [42].

Conclusions

We aimed to discover the potential drug against Coronavirus, so T-cell activation is studied with our reported compound. T-cells are a significant part of the immune system, T-cell activation enhances the immune system and can inhibit the Coronavirus. The reported Schiff base (VAP) has potential scoring function values compared with KRN7000 in 6BNK, Favipiravir, and Hydroxychloroquine in 6LU7 proteins. IC_{50} values and Lipinski's rule of five show the potential activity of VAP against covid-19. Finally, we conclude that the VAP shows excellent binding affinity, compared with the above drugs in both the immune system and against covid-19.

Acknowledgement

The authors gratefully acknowledge the financial support by the University Grants Commission, New Delhi, sanctioned in the name of UGC Block Grant by Avinashilingam Institute for Home Science and Higher Education for Women, Coimbatore, Tamil Nadu, India.

Supplementary Information

CCDC 1900253 contains the supplementary crystallographic data for this paper, and structural data is published in CSD Communications 201943. These data can be obtained free of charge *via* https://www.ccdc.cam.ac.uk/structures/ or by emailing data_request@ccdc.cam.ac.uk or contacting The Cambridge Crystallographic Data Centre, 12 Union Road, Cambridge CB2 IEZ, UK, fax: +44(0)1223-336033.

References

1 Abu-Dief A M & Mohamed M A I, *Int J Basic Appl Sci*, 4 (2015) 119.
2 Shalin K, Dhar D N & Saxena P N, *J Sci Ind Res*, 68 (2009) 181.
3 Manjula B, Antony S A & Dhanaraj C J, *Spectrosc Lett*, 47 (2014) 518.
4 Anupama B, Sunita M, Shiva Leela D, Ushaiah B & Gyana Kumari C, *J Fluoresc*, 24 (2014) 1067.
5 Kumar V Y, Rathish N, Mayur S, Shipra B & Chanda S, *J Serb Chem Soc*, 69 (2004) 991.
6 Kajal A, Bala S, Kamboj S, Sharma N & Saini V, *J Catal*, 2013 (2013) 1.
7 Brodowska K & Lodyga-Chruscinska E, *Chemik*, 68 (2014) 129.
8 El-Bindary A A, El-Sonbati A Z, Diab M A, & Abd El-Kader M K, *J Chem*, (2013) 1. http://dx.doi.org/10.1155/2013/682186.
9 Mahalingam V, Chitrapriya N, Frank R, Fronczek & Natarajan K, *Polyhedron*, 29 (2010) 3363.
10 Gupta K C & Sutar A K, *Coord Chem Rev*, 252 (2008) 1420.
11 Gowri M & Daniel T, *Mol. Cryst Liq Cryst*, 606 (2015) 199.

12 Gowri M & Jayabalakrishnan C, *Int J Appl Biol Pharm*, 3 (2012) 327.
13 Mohanram I & Meshram J, *Int Sco Res Not*, (2014) 7. (https://doi.org/10.1155/2014/639392).
14 Kadhim S, Abd-Alla I Q & Hashim T J, *Int J Chem Sci*, 15 (2017) 1.
15 Suresh M S & Prakash V, *Phys Sci Int J*, 5 (2010) 2203.
16 Suresh M S & Prakash V, *E J Chem*, 8 (2011) 1408.
17 Chandra S, Jain D, Sharma A K & Sharma P, *Molecules*,14 (2009) 174.
18 Kumar K V, Sunand K, Ashwini K, Kumar P S, Vishnu S & Samala A, *J Appl Pharm Sci*, 2 (2017) 8.
19 Kurdekar G S, Sathisha M P, Budagumpi S, Naveen V Kulkarni, Vidyanand Revankar K & Suresh D K, *Med Chem Res*, 21 (2012) 2273.
20 Gowri M, Saranya B & Athimoolam S, *Indian J Chem*, 60B (2021) 1110.
21 Beaudry F, Ross A, Lema P P & Vachon P, *Phytother Res*, 24, (2010) 525.
22 Kumar R, Sharma P K & Mishra P S, *Int J Pharmtech Res*, 4 (2012) 266.
23 Singh N, Hingorani S, Srivastava J, Puri V & Agarwala B V, *Synth React Inorg Met Org Chem*, 22 (1992) 1283.
24 Bruker, SMART Bruker AXS Inc., Madison, Wisconsin, USA, 2001.
25 Pahontu E, Proks M, Shova S, Lupascu G, Ilies D C, Barbuceanu S F, Socea L I, Badea M, Paunescu V, Istrati D, Gulea A, Draganescu D & Pirvu C E D, *Appl Organometal Chem*, 33 (2019) 1.
26 Deepak, Chauhan S, Verma K K & Garg S, *Chem Sci Trans*, 6 (2017) 448.
27 Sheldrick G M, *Acta Crystallogr C*, 7, (2015) 3. https://journals.iucr.org/c/.
28 Spek A L, *Acta Crystallogr D*, 65 (2009) 148.
29 Bernstein J, Davis R E , Shimoni L & Chang N L, *Angew Chem Int Ed* Engl, 34 (1995) 1555.
30 Shakeel A K, Rizwan K, Sammia S, Mahmoud A N, Rasheed T & Hira A, *Appl Organomet Chem*, 34 (2020) e5444.
31 Najlaa S, Radadi Al, Ehab M Z, Gehad G M & Hayam A A. *J Chem*, 2020 (2020). (https://doi.org/10.1155/2020/1548641).
32 Brahma V K, Thomas C & Donna L F, *J Immunity*, 48 (2018) 202.
33 Divya C, Noemi A, Saavedra A, Leandro J C, Matthew J G P, Pooja A, Tang Y, Rhys P, Hui-Fern K, Dale I G, Santosh K, Stewart K R, Srinivasan S, Jae H L, Xiangshu W, Jose A G, Weiming Y, Jamie R, Jerome Le N, Steven A P & Amy R H, *Cell Chem Biol*, 25 (2018) 571.
34 "Coronavirus disease 2019 (COVID-19)-Symptoms and causes", *Mayo Clinic*, Retrieved 14 April (2020).
35 Hui D S, Azhar E I, Madani T A, Ntoumi F, Kock R, Dar O, Ippolito G, Mchugh T D, Memish Z A, Drosten C, Zumla A & Petersen E, *Int J Infect Dis*, 91 (2020), 264.
36 Tetsuya M, *Uirusu*, 54 (2004) 97.
37 Liu W, Zhu H L & Duan Y, *Curr Top Med Chem*, 20 (2020) 8.
38 Opatz T, Senn-Bilfinger J & Richert C, *Angew Chem Int Ed*, 59 (2020) 9236.
39 Jin Z, Xiaoyu Du X, Xu Y, Deng Y, Liu M, Zhao Y, Zhang B, Li X, Zhang L, Peng C, Duan Y, Yu J, Wang L, Yang K, Liu F, Jiang R, Yang X, You T, Liu X, Yang X, Bai F, Liu H, Liu X, Guddat LW, Xu W, Xiao G, Qin C, Shi Z, Jiang H, Rao Z & Yang H, *Nature*, 582 (2020) 289.
40 Khaerunnisa S, Kurniawan H, Awaluddin R, Suhartati S & Soetjipto S, *Preprints* (2020) 1. (https://doi.org/10.20944/preprints202003.0226.v1).
41 Xing D, Yi L, Yuan-Ling X, Shi-Meng A, Jing L, Peng S, Xing-Lai J & Shu-Qun Lu, *Int J Mol Sci*, 17 (2016) 1.
42 Maryam I, Atefeh S & Asghar D, *Turk J Chem*, 39 (2015) 306.
43 Gowri M, *CSD Comm*, 2019. (http://dx.doi.org/10.5517/ccdc.csd.cc21schq).